

# Biomass combustion: relationship between pollutant formation and fuel composition

R. M. Winter<sup>1</sup>, J. Clough, B. J. Overmoe, and D. W. Pershing<sup>2</sup>

Research assistant, research assistant, research assistant, and professor of chemical engineering, respectively, Dept. of Chemical Engineering, University of Utah, Salt Lake City, Utah 84112

**ABSTRACT** *A 65-kW refractory-walled reactor was used to study biomass combustion under conditions typical of the suspension-burning phase in a spreader-stoker-fired boiler. Isothermal combustion data and nitric oxide (NO) emission rates were obtained as a function of temperature, local oxygen concentration, and vertical velocity for sized biomass fuels. Two softwoods, a hardwood, and a North Carolina peat were studied.*

*The pyrolytic C, H, and N data confirmed the overall high volatility, relative to coal, of these biomass fuels. Particulate emissions were correlated to vertical velocity and particle geometry, but were found to be relatively insensitive to combustion-zone oxygen, temperature, and biomass composition. NO emissions are strongly dependent on combustion-zone oxygen concentration and the nitrogen content of the biomass fuel. NO emissions increased dramatically with increasing excess air and increasing fuel nitrogen; however, these emissions were relatively insensitive to both temperature and moisture content.*

## KEYWORDS

Combustion  
Emissions  
Energy  
Environmental  
control  
Fuels  
Pyrolysis

Biomass fuels account for approximately 14% of the worldwide energy consumption (1). Biomass consumption in industrialized countries ranges from 1% to 3%, but in developing countries biomass supplies approximately 43% of the primary energy needs. In general, biomass fuels are derived from renewable and living resources such as grass, straw, and trees. Hogged-wood combustion is particularly prominent in lumber-producing regions, and stoker-fired boilers are the most commonly used type of combustion equipment.

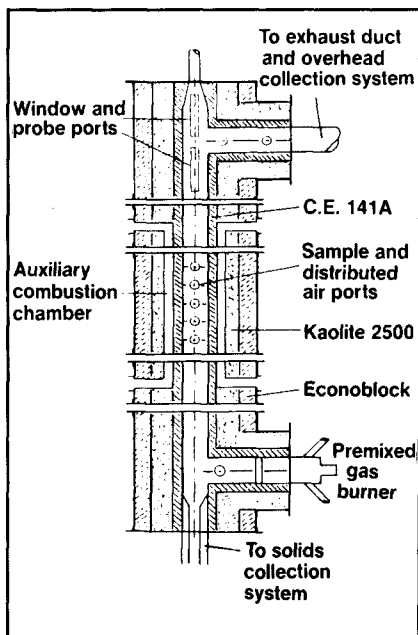
Data on the formation and control of particulate emissions from wood-fired stokers are relatively limited. Junge (2) established the importance of high excess air firing and transient combustion conditions on particulate emissions. Adams (3) used these data to develop a particulate emissions model and demonstrated that fuel feed rate, undergrate air flow rate, and fuel particle size distribution were the primary parameters affecting particulate carry-over. Kester (4) studied the combustion of hogged Douglas fir bark in a pilot-scale spreader stoker and defined NO<sub>x</sub> emission levels under normal operating conditions. Munro (5) characterized the overall influence of the combustion parameters on both NO<sub>x</sub> and particulate formation and, by inference, established the importance of the suspension-burning phase.

In a detailed study of suspension-phase burning, our objective was to quantify the relationships between (a) biomass composition and physical properties, (b) the combustion environment, and (c) the formation of pollutants. We used a 65-kW refractory-walled reactor to obtain isothermal combustion data as a function of temperature, local oxygen concentration, and vertical velocity for sized biomass fuels. Two softwoods (Douglas fir and loblolly pine), a hardwood (red alder bark), and a North Carolina peat were studied. The high-temperature combustion studies were supported by small-scale, inert pyrolysis experiments in an electric furnace.

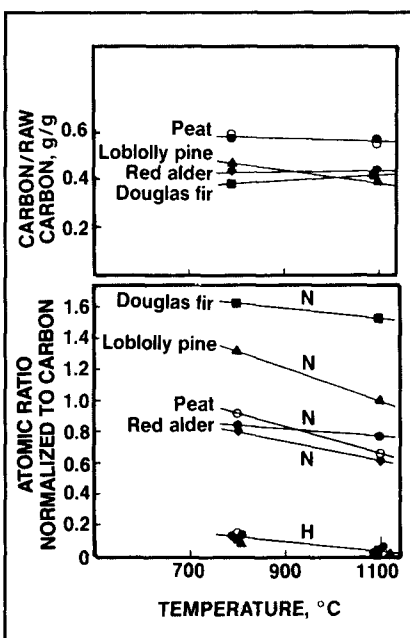
<sup>1</sup>Winter is currently an associate professor of chemical engineering with South Dakota School of Mines and Technology, Rapid City, S.D. 57701.

<sup>2</sup>Correspondence should be addressed to D. W. Pershing.

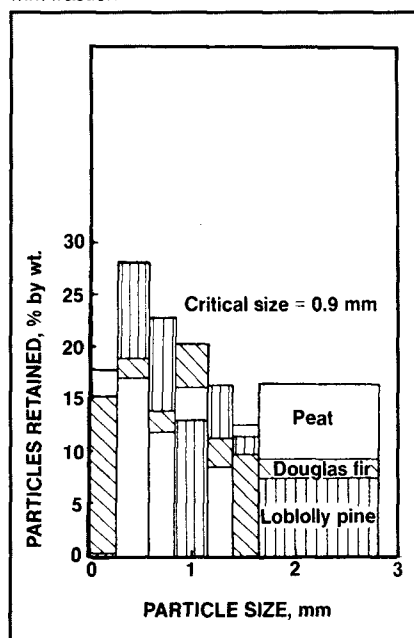
1. Suspension furnace showing the layout of the insulation



2. C, H, and N ratios vs. furnace temperature



3. Detailed size distribution data for the 0-2.8-mm fraction



## Experimental systems

### Inert pyrolysis furnace

Three-gram samples of sized biomass particles were pyrolyzed in high-temperature, carbon- and sulfur-free, ceramic boats positioned inside an electrically heated tube furnace with an inside diameter of 26 mm. Argon was used as the inert sweep gas. A pyrolysis time of 6 min was selected, based on preliminary results that defined this period as the time required to achieve asymptotic weight loss. Carbon, hydrogen, and nitrogen were measured before and after pyrolysis using a Perkin Elmer 240B C, H, and N elemental analyzer.

### Isothermal suspension furnace

Biomass combustion data were obtained in the vertical-flow, isothermal furnace illustrated in Fig. 1 (3 m × 15 cm in diameter). This furnace was designed to simulate the temperature and composition environment typical of the suspension phase in a full-scale, spreader-stoker fired boiler. The main natural gas burner (lower right) was used to provide the proper thermal and chemical environment within the reaction zone. Isothermal conditions ( $\pm 15^\circ\text{F}$ ) were maintained in the vertical portion of the furnace by firing auxiliary natural gas burners in the annulus around the main reaction chamber. Independent control of

temperature, oxygen partial pressure, and vertical velocity was achieved by varying both the firing rate and the  $\text{N}_2/\text{O}_2$  ratio of the primary natural gas burner.

The biomass feed was introduced 0.8 m above the bottom of the reaction zone, as it is done in commercial practice. Four types of behavior were exhibited, depending on the combustion conditions and on the particle size, shape, and density.

1. The feed particles fell directly to the bottom of the furnace.
2. The particles began falling, lost enough weight via dehydration to become entrained in the upward flowing combustion gases, and exited partially burned at the top of the furnace.
3. The particles became immediately entrained and burned partially prior to the exit.
4. The particles became immediately entrained and burned completely before exiting the reaction zone.

We quantified this behavior by collecting and subsequently analyzing solid samples from water-quenched traps at the bottom and top of the combustion zone (6). Carbon, hydrogen, and nitrogen analyses were performed on the samples using the Perkin Elmer 240B. The gas-phase environment at the reactor exit was

also sampled continuously and analyzed for  $\text{CO}$ ,  $\text{CO}_2$ ,  $\text{O}_2$ , and  $\text{NO}$  using infrared, paramagnetic, and chemiluminescent analyses, respectively. The temperatures at the top and bottom of the reaction zone were characterized using platinum/platinum-rhodium pyrometers.

### Experimental fuels

The proximate and ultimate analyses of the biomass fuels used in this study (Table I) indicate that the Douglas fir and loblolly pine softwoods contained relatively little nitrogen (approximately 0.2%), while the red alder bark hardwood and the North Carolina peat contained more nitrogen (0.8% and 1.2%, respectively). All of the fuels contained large amounts of oxygen, which is typical of biomass materials.

The analyses shown in Table I are on an as-received basis and indicate wide variations in initial moisture. In the combustion testing, the moisture content of each fuel was adjusted to an appropriate, constant value.

### Pyrolysis results

Initially, inert pyrolysis experiments were conducted with all of the biomass fuels to characterize the asymptotic evolution of carbon, hydrogen, and nitrogen under nonflowing, inert conditions. Figure 2 summarizes the inert pyrolysis results obtained at

### I. Fuel analyses

	Douglas fir	Loblolly pine	Red alder bark	Peat
<b>Proximate</b>				
Moisture, %	10.79	44.32	7.10	48.48
Ash, %	5.62	2.67	9.40	2.42
Volatile, %	65.07	38.61	62.10	30.99
Fixed carbon, %	<u>18.52</u>	<u>14.40</u>	<u>21.40</u>	<u>18.11</u>
	100.00	100.00	100.00	100.00
Dry-ash-free volatiles, %	77.84	72.84	74.37	63.12
Fuel value, kJ/kg	17529	11334	17873	11842
<b>Ultimate</b>				
Carbon, %	49.88	51.63	48.54	58.64
Hydrogen, %	5.54	5.63	5.49	5.12
Nitrogen, %	0.18	0.26	0.76	1.18
Ash, %	6.31	4.87	10.23	4.71
Oxygen, %	<u>38.09</u>	<u>37.61</u>	<u>34.98</u>	<u>30.35</u>
	100.00	100.00	100.00	100.00
Fuel value, kJ/kg	19645	20334	19215	22981
DMF*, kJ/kg	21085	21464	21609	24216
*DMF = dry mineral free.				

### III. Values used in computation

	$d_p,^a \times 10^{-4} m$	
	18.6	6.68
$u_{rel},^b m/s$	-0.8	.02
Residence time, s	1.15	0.51
Thermal conductivity, W/(m °C)	0.142	0.142
Convective heat transfer coef., W/(m <sup>2</sup> °C)	144	279
Thermal diffusivity, (m <sup>2</sup> /s) $\times 10^{-7}$	1.78	1.78
<b>Moduli</b>		
Fourier	0.237	0.809
Biot	0.943	0.660
Temperature ratio, ° $\theta_0/\theta_i$	0.8	0.3
Temp., °K	490	980
<small><sup>a</sup>Critical entrainment diameter. <sup>b</sup>Average relative velocity. Gas velocity was 4 m/s. <sup>c</sup>Where <math>\theta_0 = T_0 - T_\infty</math> and <math>\theta_i = T_i - T_\infty</math>. <math>T_0</math> = center temperature. <math>T_\infty</math> = environment temperature. <math>T_i</math> = initial temperature of solids.</small>		

800° and 1100°C for all of the biomass materials in the asymptotic region.

The carbon evolution data (Fig. 2A) confirm that the volatility of the wood fuels is greater than that of peat, which is in agreement with proximate analysis results (Table I, dry-ash-free volatiles). The relative insensitivity of the evolution of carbon to temperature (and extended pyrolysis time, which is not shown) supports the concept of "fixed carbon" even with these fuels. The ratio of wood fixed carbon to peat fixed carbon remained constant at 0.68 and was independent of temperature. This ratio is also observed in the results of the proximate analysis. The fixed carbon ratio according to the proximate analysis may represent a guideline for the relative reactivity of biomass fuels.

The residual char exhibited some nitrogen enrichment relative to the carbon with the low-nitrogen softwoods (Douglas fir and loblolly pine), but with red alder and peat, the nitrogen in the fuel was slightly preferentially evolved relative to the carbon. The hydrogen results show the strong preferential hydrogen evolution with respect to carbon. For

### II. Initial rates in min<sup>-1</sup>

	800°C	1000°C
Carbon	-0.93	-1.36
Hydrogen	-1.30	-1.87
Nitrogen	-1.40	-1.50
Total mass	-1.14	-1.58

the biomass materials tested, temperature exhibited a stronger influence over the evolution of nitrogen and hydrogen than it did over carbon.

Initial rates defined as the average normalized weight loss of a species over the initial 30 s of pyrolysis were obtained for Douglas fir (Table II) according to Eq. 1:

$$\text{rate} = \Delta(\text{wt. } X_i / \text{wt. } X_0) / \Delta t \quad (1)$$

where

$t$  = time

$X$  = species

wt.  $X_0$  = mass of species X at time = 0 s.

There was little enhancement in the initial rate of nitrogen evolution

with temperature, whereas the initial rate of carbon and hydrogen evolution increased by 50% as the temperature increased from 800°C to 1100°C.

### Particulate emissions

In a full-scale spreader-stoker, particulate loadings at the furnace exit are the result of complex interactions between such factors as the raw particle size, shape, and density, the fuel reactivity, the vertical velocity, the boiler thermal profile, and the local oxygen concentration. We attempted to isolate the various parameters and identify and quantify those that control the particulate emissions. In each case, commercial fuel samples were separated into fractions of different particle sizes using screens representing approximately 10–15% (by weight) of the total commercial distribution. The smallest two fractions (0–2.8 mm and 2.8–4.0 mm) were studied extensively because preliminary testing indicated that biomass particles of greater than 4.0 mm fell to the grate essentially unreacted.

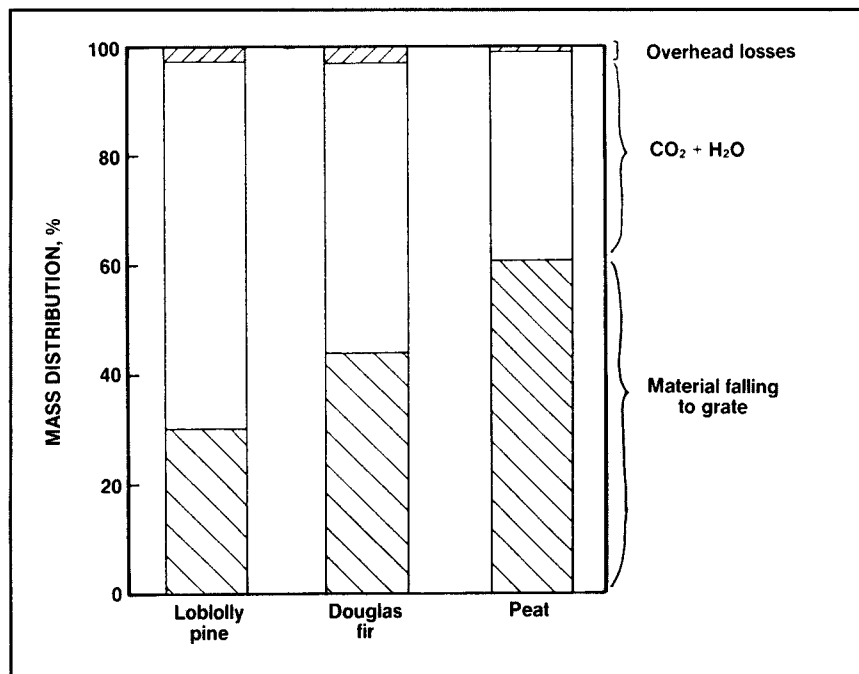
4. Mass distribution vs. fuel type (0 < diameter < 2.8 mm, 6% O<sub>2</sub>, 4 m/s, 45% moisture)

Figure 3 illustrates the detailed size distribution for the fraction of smallest size (<2.8 mm). Because of both inherent fuel differences and differences within the commercial preparation processes for softwoods and peat, considerable variations were found within each particular fraction. Figure 3 shows that the Douglas fir fines (particles <2.8 mm) included a high weight percent of small particles (<1 mm), while the peat included a large fraction of relatively larger particles. The loblolly pine distribution contained a major percentage of particles near 1.33 mm, the theoretical size for particle entrainment under the conditions used in these tests.

Figure 4 shows the fate of the biomass particles under normal commercial operating conditions (6% excess O<sub>2</sub>, 4 m/s, 45% moisture). The upper hatched region represents the entrained char material that exited the top of the combustion zone (uncontrolled particulate). The lower hatched area represents the material that fell to the bottom of the combustion zone (representing those particles which would fall to the grate in a commercial stoker). The difference represents the fraction of the initial mass that burned. Figure 4 indicates

that the combustion behavior is apparently a function of fuel type, but in all cases a significant portion of even this smallest size fraction (0–2.8 mm) fell to the grate. Similar results for the next smallest size fraction (2.8–4.0 mm) indicated that most of the mass fell to the grate with all fuels.

Figure 5 indicates that both the fraction leaving the furnace unburned and the fraction of the initial mass that falls to the grate can be correlated based on theoretical principles. Physical inspection of the sized particles indicated that the softwoods (Douglas fir and loblolly pine) were relatively flat and rectangular in shape, while the red alder bark and peat were more nearly spherical.

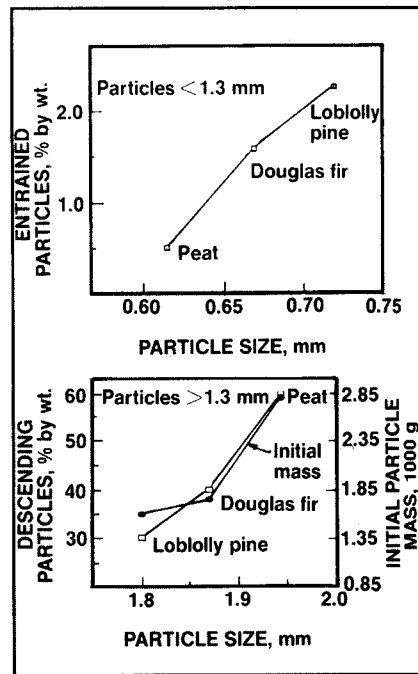
The drag coefficient was estimated to be 2.6, and the corresponding critical entrainment diameter was 1.33 mm, assuming that the drag and buoyant forces were equal to the gravity force:

$$d_p = U_t^2 + 3C_d \rho_g / [4g(\rho_p - \rho_g)] \quad (2)$$

where

$$d_p = \text{critical entrainment diameter}$$

5. The impact of particle size distribution on entrainment, showing (top) the fraction that leaves the furnace unburned and (bottom) the fraction that falls to the grate.

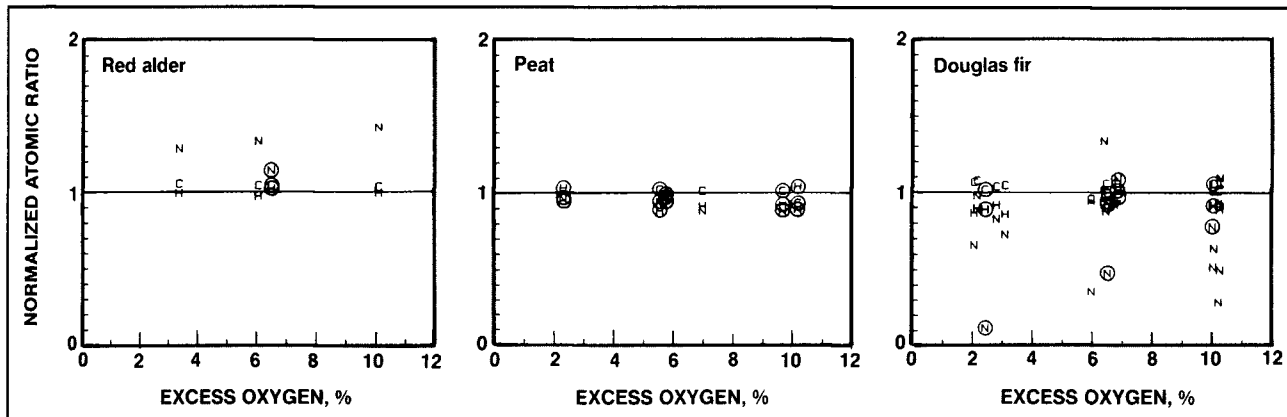


- $U_t$  = terminal velocity
- $C_d$  = drag coefficient
- $\rho_g$  = density of the fluid
- $\rho_p$  = density of the particle
- $g$  = local acceleration due to gravity.

Based on a critical particle diameter of 1.33 mm and the detailed mass distribution data (Fig. 3), mean particle diameters of the falling material (>1.33 mm) and the entrained material (<1.33 mm) were calculated for each fuel.

Curve A of Fig. 5 shows that the unburned losses correlate well with the mean size of the entrained material. The loblolly pine losses were highest because this fuel contained the highest mass fraction of particles small enough to be entrained but large enough to avoid complete oxidation within the residence time. Conversely, the fraction of material falling to the furnace bottom (Curve B) was highest with the peat.

We made a comparison of the mass and size distribution above the critical particle diameter for each fuel. These analyses showed that the peat fuel contained a greater proportion of large-diameter particles than the



Douglas fir and loblolly pine. For the nominal particle size segment of 2.225 mm, the peat contained 45% greater mass than the Douglas fir and 55% more mass than the loblolly pine. The mass of a particle of a given diameter and density can be represented as:

$$m_p = \rho_p (\pi D_p^3 / 6) \quad (3)$$

where

- $m_p$  = mass of a particle
- $D_p$  = particle diameter
- $\rho_p$  = density

From Eq. 3, we can see (Curve C of Fig. 5) that the curvature observed in Curve B is primarily a function of the particle diameter. Particle density also influences Curve B, as indicated in Eq. 3. The density of peat is typically 50% greater than the density of wood; therefore, the density strongly impacts the relative particle masses.

These data demonstrate that to accurately predict entrainment and grate loadings in a practical combustion environment, it is essential to have detailed, high-resolution particle-size data near the critical entrainment size. With biomass fuels, unburned losses are not critically dependent on chemical parameters. Any effects of increased hydrocarbon volatility with the softwoods relative to peat were completely masked by small differences in the details of the particle size distribution.

Figure 6 shows the fate of the fuel

carbon, hydrogen, and nitrogen for the particles (<2.8mm) that descended (grate material) through the combustion zone which was maintained at 1000°C. The figure includes data for both high and low moisture contents with the Douglas fir, red alder, and peat fuels. The data are reported as atomic ratio relative to carbon (normalized with respect to the atomic ratio in the raw feed material) as a function of the oxygen partial pressure in the reactor. The carbon and hydrogen in the collected solids were essentially identical to the raw fuels (with ratios near 1.0), indicating that the material that fell to the furnace bottom was essentially unreacted. Neither oxygen partial pressure nor moisture had any significant effect on the fate of the material which fell to the grate. Nitrogen was slightly preferentially retained relative to carbon with the red alder bark and preferentially evolved with the Douglas fir, suggesting slight differences in the speciation of the most volatile nitrogen components.

Figure 7 shows complementary results for the solid material collected at the furnace exhaust (entrained particles which did not completely burn). The hydrogen was almost totally evolved from these samples, indicating extensive devolatilization. As in the inert pyrolysis results (Fig. 2), the hydrogen evolution was highly preferential relative to the total carbon. In all cases, the nitrogen evolution was at least as great as that of carbon. With the Douglas fir particles, the nitrogen was almost

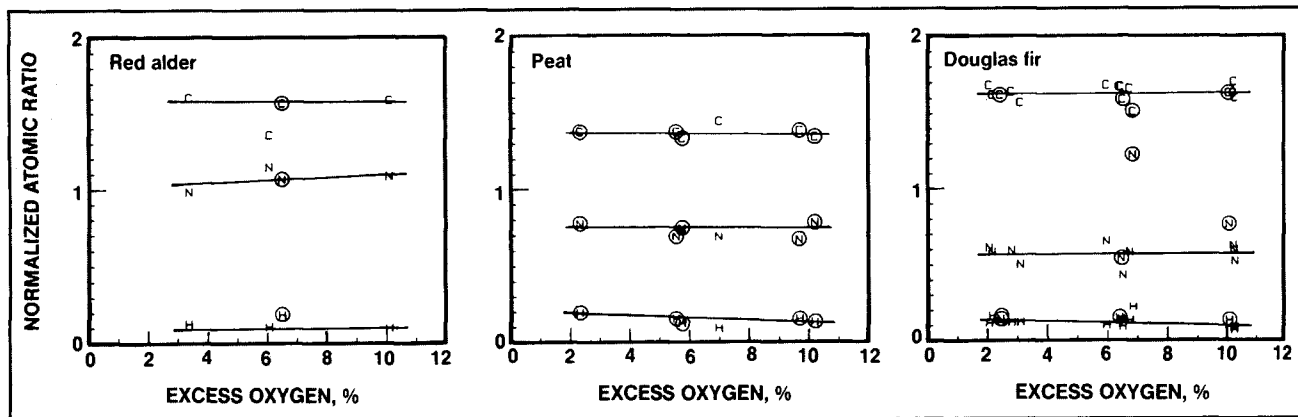
completely evolved. Again, oxygen partial pressure and moisture appear to have little effect on the extent of C, H, and N evolution.

Comparison of the N/C ratios for the Douglas fir under inert pyrolysis conditions (Fig. 2) and oxidative conditions (Figs. 6 and 7) indicates the only apparently anomalous behavior. The nitrogen evolution ratios are considerably lower for the oxidative cases than for the inert pyrolysis cases, suggesting that oxygen enhances some nitrogen evolution relative to carbon. Perhaps this effect is pronounced with the Douglas fir because of the flat particle geometry and large portion of exposed relative surface area.

The average relative velocity ( $u_{rel}$ ) can be obtained for the ascending and descending particles by rearranging Eq. 2. Using  $u_{rel}$ , a surface-convective heat-transfer coefficient ( $h$ ) and the residence time ( $\tau$ ) were calculated for each category of particle. As a first approximation, an analysis for lumped heat capacity was formulated, which necessitated the computation of the Biot and Fourier moduli. Using the Heisler charts (7), the center temperature was computed for a biomass particle based on a spherical geometry.

Table III gives the values of the particle properties used in the computation and the results. The residence time for a descending particle was approximately twice as long as that of an average entrained particle. The descending particle had a surface-convective heat-transfer coefficient that was 0.5 of that of an

7. Overhead C, H, and N vs. excess oxygen. (Circled points are at 45% moisture content; others are at 15% moisture content)



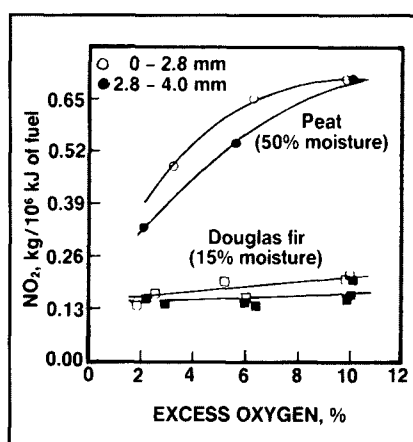
entrained particle. Thus, the lumped-heat-capacity analyses showed that the average descending particle would reach a maximum temperature of 490°K, while the average entrained particle would obtain a centerline temperature of 980°K.

These first-approximation analyses agree well with the data represented in Figs. 6 and 7. Those particles which descended to the bottom of the furnace achieved a relatively low temperature, which resulted in minimal devolatilization of the descending particle. The entrained particle devolatilized and burned rapidly as its temperature rose to nearly that of the surrounding atmosphere.

In summary, the particle size distribution plays a key role in particle entrainment and hence in particulate emissions. Neither local oxygen availability nor fuel moisture appear to strongly influence the selective evolution of C, H, or N. Particles large enough to avoid entrainment reach the grate essentially unreacted. The unburned particles being carried out of the combustion zone with flue gases are made up primarily of carbon; consequently, these will be difficult to oxidize further even with "fly ash reinjection." Fuel moisture, however, does contribute strongly to the fuel density and thermal conductivity (8).

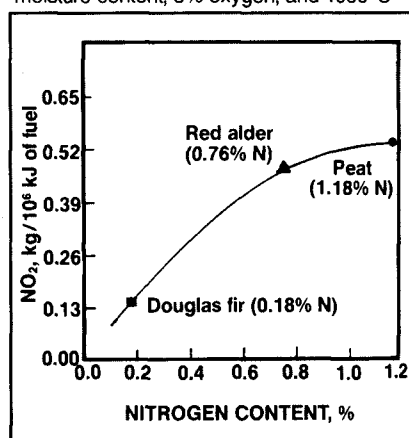
### NO<sub>x</sub> emissions

Previous studies on NO<sub>x</sub> emissions from solid and liquid fossil fuels (9, 10) have indicated that NO formation is controlled by thermal history, local

8. NO<sub>x</sub> emissions vs excess oxygen (1000°C)

oxygen availability, fuel nitrogen content, overall fuel composition, and particle size. Figure 8 summarizes our data on NO formation as a function of local oxygen partial pressure for both the Douglas fir and peat at 1000°C with the two fractions of smallest size. The emissions for the peat are higher because of the higher original fuel nitrogen. Increasing overall excess oxygen increased the emissions in both cases. The smaller particles produced slightly higher NO emissions, in agreement with previous results on pulverized coal (9).

The increased NO formation at high local oxygen concentrations was apparently the result of increased oxygen atom availability, not enhanced fuel nitrogen evolution; in all cases, 95% of the fuel bound nitrogen was evolved from the entrained particles. For the Douglas fir, the conversion of the evolved nitrogen increased from 40% to 70% when the

9. NO<sub>x</sub> emissions vs nitrogen content at 15% moisture content, 6% oxygen, and 1000°C

oxygen was increased from 2% to 10%. With the North Carolina peat, the corresponding increase in the conversion of the evolved nitrogen was 20% to 40%. The maximum emissions for Douglas fir and North Carolina peat are respectively 0.14 kg/10<sup>6</sup> kJ (0.32 lb/10<sup>6</sup> Btu) and 0.75 kg/10<sup>6</sup> kJ (1.7 lb/10<sup>6</sup> Btu) and are based on the dry-ash-free energy content of the fuel.

Figure 9 shows the overall effect of fuel nitrogen content on exhaust NO emission. As expected, the NO emissions increased with increasing fuel nitrogen content, and the increase was nonlinear because the percent conversion of the evolved nitrogen decreased at the higher nitrogen levels. This trend is in good agreement with those observed previously for both liquid and solid fuels (9, 10) and is believed to result from the inherently second order nature of the N<sub>2</sub> formation reactions. The maximum emission for the red alder

fuel was 1.3 kg/10<sup>6</sup> kJ (3.02 lb/10<sup>6</sup> Btu). In Fig. 9, the parentheses contain the percent of fuel nitrogen.

Emissions data were also obtained with red alder at 800°, 1000°, and 1200°C with both 10% and 45% moisture contents. These data showed that neither temperature nor moisture content had a significant effect on the conversion of evolved nitrogen to NO over the range studied. In each case, the percent conversion of the evolved nitrogen to NO was 30 ± 2%.

In summary, the key parameters controlling NO<sub>x</sub> formation in the suspension phase are fuel nitrogen content and overall excess oxygen. Temperature and moisture content are not of first-order importance. Under normal commercial combustion conditions, suspension-phase fuel nitrogen conversions as high as 70% can be expected with low-nitrogen, hogged woods. Particle size distribution has only a slight influence on NO formation in the suspension phase, but it can have a strong influence on overall emissions because it controls the fraction of the particles that fall to the grate. In previous work (5), the conversions of fuel nitrogen during grate combustion were shown to be lower than the conversions during suspension-phase combustion.

## Conclusions

The pyrolytic C, H, and N data confirm the overall high volatility of all of the biomass fuels studied relative to coal. The carbon and hydrogen evolution trends directly paralleled those observed in the combustion experiments. Hydrogen evolution is rapid and essentially complete. Only nitrogen evolution exhibited major differences between fuels; the softwoods contained less total fuel nitrogen, but that nitrogen was more refractory relative to carbon than in the case of the hardwood and peat.

Particulate emissions attributable to suspension-phase processes are directly related to entrainment; therefore, vertical velocity and particle size are of first-order importance. Unburned carbon carry-over can be correlated in terms of the mean size of the particles smaller than the critical entrainment diameter, as predicted by theoretical fluid

mechanics. Likewise, the fraction of the initial feed which will reach the grate essentially unburned correlates with the amount of material larger than the critical entrainment diameter. Thus, fuels which contain a significant fraction of particles just slightly smaller than the critical entrainment diameter should produce emissions high in particulates.

The lumped-heat-capacity analysis supports these conclusions and emphasizes the strong role that particle mass and size distribution plays in the combustion of biomass in the suspension phase. Biomass physical properties such as density, thermal conductivity, and size distribution strongly influence the fate of particles injected into a dynamic combustion zone. Particulate carry-over is relatively insensitive to combustion-zone oxygen, temperature, and biomass composition; however, combustion-zone oxygen and temperature do strongly influence the percent of incoming particles that are entrained and are subsequently burned.

Nitric oxide emissions are a strong function of combustion-zone oxygen concentration and fuel nitrogen content. With all of the fuels studied, over 95% of the fuel nitrogen was evolved from those particles which were entrained. NO emissions increased dramatically with increasing overall excess air as a result of increased local O<sub>2</sub> availability. NO emissions also increased with increasing fuel nitrogen; however, this effect is nonlinear because of decreased fuel nitrogen conversions at high fuel nitrogen concentrations. NO emissions were relatively insensitive to both temperature and moisture content. Changes in overall particle size distribution alter the suspension vs. the bed burning split but have relatively little direct impact on suspension-phase NO formation. □

## Literature cited

1. Hall, D. O., Barnar, G. W., and Moss, P. A., *Biomass for Energy in the Developing Countries*, Pergamon Press, Oxford, England, 1982.
2. Junge, D. C., *Boilers Fired with Wood and Bark Residues*, Research Bulletin 17, Oregon State University, 1975.
3. Adams, T. N., *Combustion and Flame* Vol. 39, pp. 225-239.
4. Kester, R. A., *Nitrogen dioxide emissions from a pilot plant spreader stoker bark fired boiler*, Ph.D. dissertation, University of Washington, Seattle, 1980.
5. Munro, J. M., Bradshaw, F. W., and Pershing, D. W., *Control of pollutant emissions from coal and wood combustion in spreader-stoker systems*, paper presented at the 1982 AFRC International Symposium on Conversion to Solid Fuels, International flame research foundation, IJ muiden, Holland, 1982.
6. Winter, R. M., *Optimization of wood combustion and control of NO<sub>x</sub> formation in the suspension phase of a spreader-stoker furnace*, Ph. D. dissertation, University of Utah, Salt Lake City, 1986.
7. Heisler, M. P., *Temperature Charts for Induction and Constant Temperature Heating*, Trans. ASME 69: 227(1947).
8. Tillman, D. A., Rossi, A. J., and Kitto, W. D., *Wood Combustion: Principles, Processes, and Economics*, Academic Press, New York, 1981.
9. Chen, S. L., Heap, M. P., Pershing, D. W., and Martin, G. B., *Influence of coal composition on the fate of volatile and char nitrogen during combustion*, Nineteenth International Symposium on Combustion, The Combustion Institute, Pittsburgh, 1983.
10. England, G. C., Heap, M. P., Pershing, D. W., Nikart, R. K., and Martin, G. B., *Mechanisms of NO<sub>x</sub> formation and control: alternative and petroleum-derived liquid fuels*, Eighteenth International Symposium on Combustion, The Combustion Institute, Pittsburgh, 1981.

This research was supported by Weyerhaeuser Corp. We gratefully acknowledge the guidance and encouragement of the project supervisors, Terry Adams and Robert Spurell. We sincerely appreciate the technical advice of David Tillman, EnviroSphere, and Ken Ragland, University of Wisconsin.

Received for review May 19, 1988.

Accepted July 15, 1988.